Energy & Environmental Science

Accepted Manuscript

ROYAL SOCIETY OF CHEMISTRY

www.rsc.org/ees

Perovskite Photovoltaics: Life-Cycle Assessment of Energy and Environmental Impacts

Jian Gong,[a] Seth B. Darling[b,c] and Fengqi You[a*]

a Northwestern University, Department of Chemical and Biological Engineering, 2145 Sheridan Road, Evanston, IL, 60208, USA

b Argonne National Laboratory, Center for Nanoscale Materials, 9700 South Cass Avenue, Argonne, IL, 60439, USA

c University of Chicago, Institute for Molecular Engineering, 5801 South Ellis Avenue, Chicago, IL, 60637, USA

April 21, 2015

Submitted to *Energy & Environmental Science*

Abstract

The past few years have witnessed a rapid evolution of perovskite solar cells, an unprecedented photovoltaic (PV) technology with both relatively low cost and high power conversion efficiency. In this paper, we perform a life cycle assessment for two types of solution-processed perovskite solar modules to shed light on the environmental performance of this promising class of PVs. One module is equipped with FTO glass, gold cathode, and mesoporous TiO_2 scaffold; the other is equipped with ITO glass, silver cathode, and ZnO thin film. We develop comprehensive life cycle inventories (LCI) for all components used in the modules. Based on the LCI results, we conduct life cycle impact assessment for 16 common life cycle impact indicators, Eco-indicator 99, and two sustainable indicators: energy payback time (EPBT) and CO_2 emission factor. We compare the results of Eco-indicator 99, EPBT, and CO_2 emission factor among existing PV technologies, and further perform uncertain analysis and sensitivity analysis for the two modules. The results demonstrate that perovskite solar modules possess the shortest EPBT, and future research should be directed to improving system performance ratio and device lifetime,

* To whom all correspondence should be addressed. Phone: (847) 467-2943; Fax: (847) 491-3728; E-mail: you@northwestern.edu

and reducing precious metal consumption and energy-intensive operations in order to lower the CO_2 emission factor.

Key words: perovskite solar cells, life cycle assessment, uncertainty analysis, photovoltaics.

1. Introduction

Efficiently converting solar energy to electricity, photovoltaic (PV) technologies are gaining substantial attention due to their unrivalled potential for large-scale renewable energy production and greenhouse gas (GHG) emissions reduction. Although currently a small contributor to global electricity production, PV installations have rapidly increased over the past decade, and this industry is expected to be a major player in the electricity market in the long term. One important factor that impedes the expansion of PV technologies is the high electricity production cost compared to those of fossil fuels.[1] Researchers have tried a variety of materials and even envisioned new PV architectures to address the cost-and-efficiency dilemma. The first generation of PVs technologies utilizes wafer-based crystalline silicon as the active material; later in the second generation, the active material is replaced with thin-film semiconductors, often applied via vapor deposition techniques; production cost is projected to be further reduced using organic semiconductors and solution-processing methods in the third generation.[2]

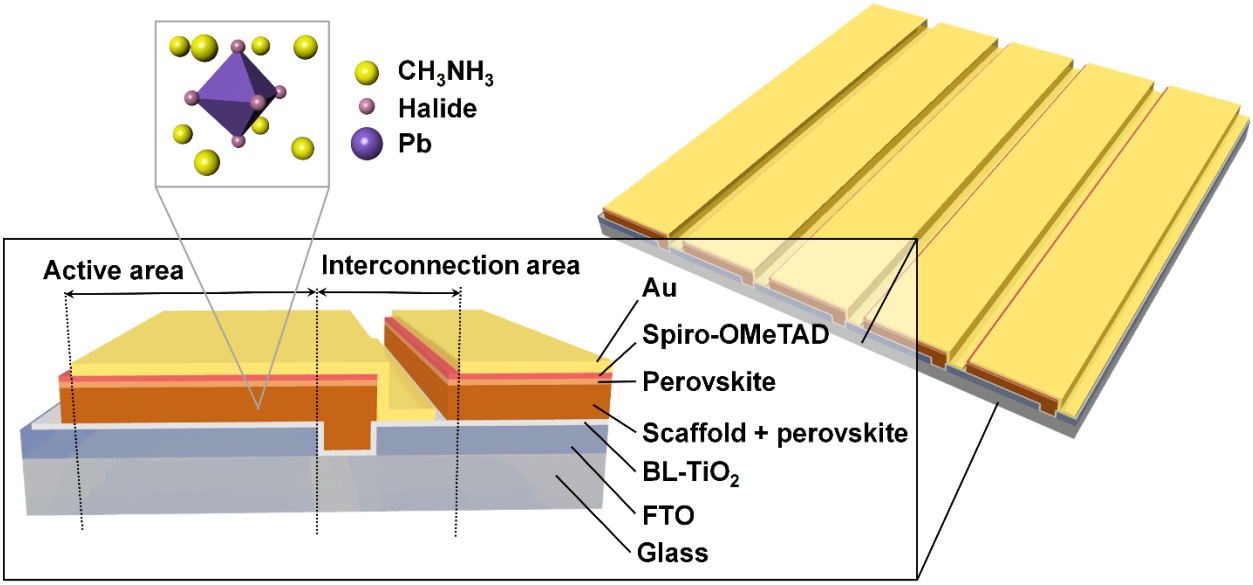

Figure 1. A perovskite solar module.

Over the past few years, an emerging perovskite PV technology unexpectedly burst on the scene with both low cost and remarkably high efficiency.[3] An illustration of such a perovskite solar module is shown in Figure 1. The efficiency of perovskite solar cells has surged from 3.8% to 20.1% in just five years, and will likely continue to climb toward 25% in the future.[4] Developing effective and efficient perovskite solar cells has become a dynamic research field. In addition to the study of perovskite materials,[5] researchers have attempted various components and processing techniques for perovskite solar cells. For instance, silver and gold are applied as electrode materials;[6-8] P3HT and spiro-OMeTAD are used as hole transporters;[9, 10] TiO_2 and Al_2O_3 are demonstrated as the porous scaffold;[2, 8, 11] although perovskites were originally used as sensitizers in dye-sensitized solar cells, researchers are now applying thin-film perovskite structures and achieving excellent results.[2, 6, 12] With respect to the thin-film photovoltaic devices, existing lab-scale processing techniques include solution deposition,[6] vacuum deposition,[13] and vapor-assisted solution deposition.[7, 14] With the ultimate goal of commercial viability, perovskite solar cells processed with solution deposition techniques are favorable due to the low-temperature conditions and low energy consumption.[15] The introduction of a sequential method to the solution deposition techniques permits better control over the perovskite morphology, thus increasing the reproducibility of the performance.[16-18] Priority in the recent advancement of perovskite solar cells is given to developing new devices with the highest possible power conversion efficiencies. However, foreseeable environmental threats, most notably climate change caused by the intensive energy consumption during manufacturing, and ecotoxicity caused by the use of rare and poisonous metals, may unfortunately hinder perovskite PVs from becoming a thriving energy technology. Therefore, a thorough environmental evaluation for this PV technology is indispensable to identify environmental hotspots and propose effective mitigation strategies.

Life cycle assessment (LCA) is a widely used methodological framework for estimating and assessing the environmental impacts attributable to the life cycle of a product.[19] LCA helps identify the key contributors of a product to numerous impact categories and has been introduced to evaluate the environmental performance of a wide array of PV technologies. In addition to the life cycle impact indicators in common LCA studies, one of the most widely used sustainability indicators to compare among the PVs is energy payback time (EPBT), which quantifies the time necessary for a PV device to generate equivalent energy that is consumed to produce it. Silicon-

based PVs were among the earliest technology to directly convert sunlight to electricity. A crystalline silicon module is evaluated with an EPBT of 3 to 4 years.[20] Amorphous silicon can be deposited in thin films at relatively low temperatures and significantly reduce the EPBT to 1.1 years in the common Mediterranean climate condition.[21] In the same paper, a comparative study shows that cadmium telluride (CdTe) thin-film PV module not only has lower production cost, but also achieves a shorter EPBT of 0.9 years. Another class of well-known thin-film PVs is made of copper indium diselenide, or CIS, which owns an EPBT of 1.9 years.[22] Organic PVs (OPV) is a recently developed technology using cost-effective polymer as the active layer. It was the major player in the research of PV materials before the advent of perovskite. Numerous methods have been proposed to reduce the cost and energy burden of manufacturing an OPV module.[23] A recent study for an OPV of 0.5% power conversion efficiency concludes with an EPBT of 1.42 years. Increasing conversion efficiency and improving module stability are regarded as the challenges of this technology.[24] There are more analyses for silicon PVs,[25-27] CdTe PVs,[22, 26, 28-31] CIS PVs,[20, 22] and OPVs,[23, 29, 32-36] each with different conditions and assumptions. Comprehensive comparisons have been made among various PV technologies with diverse temporal and geographical conditions.[36-38] A Monte Carlo simulation method was also applied for calculating the levelized cost of energy for PVs.[39] None of the existing articles, however, apply life-cycle thinking and tools to perovskite PV systems.

In this work, we perform a cradle-to-grave LCA to evaluate the environmental impacts of two solution-processed perovskite solar modules. We conduct life cycle impact assessment for 16 midpoint impact categories and generate endpoint results according to the Eco-indicator 99 methodology. We also calculate EPBT and CO_2 emission factor, the latter of which equals the carbon footprint per kWh electricity generated, and compare the results with existing PV technologies in order to place this technology in the context of proven technologies. Furthermore, since the life cycle inventories (LCI) are developed based heavily on stoichiometric relationships and several parameters are inherently unstable, we perform uncertainty analysis of EPBT and CO_2 emission factor with respect to the uncertainties in primary energy consumption, carbon footprint, performance ratio, module efficiency, insolation, and lifetime. Based on the uncertainty analysis, we conduct a series of sensitivity analyses and identify the most influential parameters. The results provide guidance to the development of perovskite solar cells for more environmentally sustainable systems.

The paper is organized as follows. In the next section, we present the materials and methods following the standard procedure of an LCA. The goal and scope definition introduces the functional unit, system boundary, technical differences between the two perovskite solar modules, and data accuracy. Next, in LCI analysis we provides detailed mass and energy inventories. Later, life cycle impact assessment covers the results for 16 impact categories, Eco-indicator 99, and two sustainability indicators, followed by uncertainty analysis and sensitivity analysis. The life cycle interpretation is incorporated into the previous life cycle phases. Finally, we discuss the LCA results and provide insights into sustainable perovskite solar modules.

2. Materials and methods

2.1. Goal and scope definition

The goal of this study is to assess the potential life cycle impacts of two perovskite solar modules. The functional unit of this LCA is defined as 1 m^2 of the perovskite solar module, and all of the inventories generated are converted aligning with the functional unit. The functional unit is not selected as unit power generation to avoid the introduction of external parameters such as isolation.[21]

This study is a cradle-to-grave LCA, whose system boundary is illustrated in Figure 2. There are four life cycle stages: (1) component production; (2) module manufacturing; (3) module use; (4) disposal. The first stage starts from raw materials extraction to produce the components used in the second stage. In the second stage, the PV module is assembled by depositing the components onto the substrate. The manufacturing process consumes energy and lets off emissions. After the PV module is utilized and decommissioned, the waste modules are landfilled in the disposal stage. Other disposal methods, such as incineration and waste recycling, are not considered in the system, because there is a lack of data about combusting or recycling waste perovskite modules. We exclude module use and transportation from the system boundary; this assumption is applied in a number of LCA studies for PV technologies.[32-34, 38] Balance of system is omitted in the system boundary so that the results can be directly compared with those of other PV technologies.

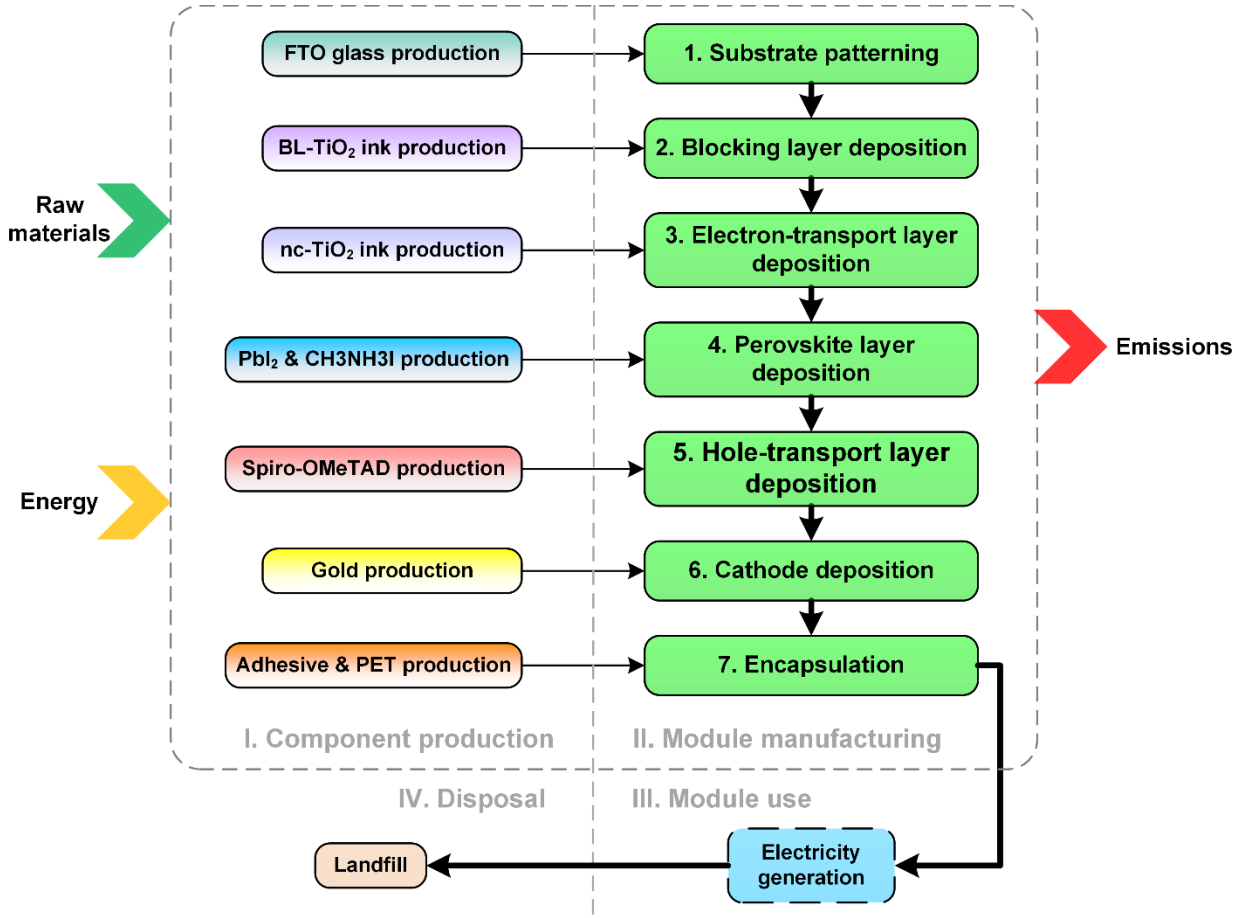

Figure 2. System boundary of manufacturing a perovskite solar module with mesoporous TiO_2 scaffold. Only major components are demonstrated in the component production stage.

Various device architectures have been reported for perovskite PVs. In this analysis, we will focus on two representative solution-processed perovskite solar modules. The major differences between the TiO_2 module and the ZnO module are listed in Table 1.

Table 1 Differences between two perovskite solar modules.

	TiO_2 module[10]	ZnO module[6]
Module efficiency	9.10%	11.0%
Substrate	FTO glass	ITO glass
Electron-transport layer	Mesoporous TiO_2 scaffold	ZnO thin film
Cathode	Gold	Silver
Blocking layer	Required	Not required
Sintering after deposition	Required	Not required

As depicted in Figure 1, the procedure for manufacturing a TiO_2 module involves seven steps.[10] In the first step, fluorine doped tin oxide (FTO)-coated glass substrates are patterned with a raster

scanning laser and then cleaned with deionized water and ethanol in an ultrasonic bath. Later, silver paste is screen-printed on the interconnection area between the cells. The substrates are sintered to form a metallic mask. In the second step, a blocking layer of TiO_2 is deposited onto the substrates using spray pyrolysis, followed by lifting off the metallic mask and cleaning the surface of the substrates. In step three, a TiO_2 scaffold layer is screen-printed before the substrates are sintered to form a nanocrystalline mesoporous layer. In steps four and five, a perovskite layer and a hole-transport layer are deposited on the substrates. In order to form a perovskite active layer, PbI_2 is spin-coated on the substrates, which are later sintered for one hour and dipped in a CH_3NH_3I/isopropanol solution. Subsequently, spiro-OMeTAD, the hole-transport material, is spin-coated on top of the perovskite layer. A green Nd:YVO_4 laser is employed to etch the perovskite and spiro-OMeTAD layers from the interconnection area. In step six, a gold electrode is deposited over the hole-transport layer using thermal evaporation. Finally, the module is completed by encapsulating the substrates in step seven.

In the second module architecture, a ZnO module replaces the mesoporous TiO_2 scaffold with a thin film of ZnO nanoparticles. The modification not only helps eliminate the blocking layer deposition (step two) and energy-intensive sintering operations, but also effectively improves the cell efficiency to 15.7%.[6] Although this manufacturing technique demonstrates great potential for reducing production cost and environmental burden, high-performing results are only reported for solar cells rather than scalable solar modules. In order to explore the capability of perovskite solar modules, we assume ZnO modules fabricated using this technique maintain the same cell efficiency and have an active area ratio of 70.0%, resulting in a module efficiency of 11.0%. The system boundary of manufacturing a ZnO module is similar to Figure 2, while step two is omitted, and the substrate, electron-transport layer, and cathode are changed to indium tin oxide (ITO)-coated glass, ZnO thin film, and silver, respectively.

Data used in this LCA come from literature and quantitative estimates. If the characterization factors of a material can be found in Ecoinvent database,[40] these data are extracted and used in life cycle impact assessment. Accordingly, the data accuracy of these characterization factors is high. Otherwise, we develop a process to evaluate the characterization factors of this material from raw materials that are reported in Ecoinvent. The LCI's of these processes are based on stoichiometric relationships, solubility, yields, split fractions, and energy consumption reported in the literature. The accuracy of these LCI's is high. For several module-related parameters that are not reported

in the literature, or are inherently uncertain, but reported with average values, we give conservative estimates or apply the average values. The data accuracy of these parameters is low. We assign distributions to these parameters and examine the influence of the uncertainties on the results in uncertainty analysis.

2.2.Life cycle inventory analysis

Inventory analysis is of central role in an LCA. Based on the system boundaries described above, we classify the LCI of each module into two categories: material inventory and energy inventory.

A material inventory table consists of the mass of raw materials, direct emissions during manufacturing, and disposal materials per functional unit of the module. The material inventory of 1 m^2 of the TiO_2 module is shown in Table 2. The active area ratio and module efficiency are 70.0% and 9.10%, respectively.[10] The mass for the cleaning solvents, adhesive and polyethylene terephthalate (PET) are extracted from the literature.[23, 34, 41] The mass of blocking layer (BL)-TiO_2 ink, nanocystalline (nc)-TiO_2 ink, PbI_2, CH_3NH_3I, spiro-OMeTAD, and gold are derived based on the thickness of the corresponding layers, the active area ratio of the module, and the material utilization efficiency; the mass of dimethylformamide, isopropanol, and chlorobenzene are calculated according to the concentrations of corresponding solutions. Since the material utilization efficiencies are not reported for perovskite PV modules, we assume that the material utilization efficiencies for spin-coating, spray pyrolysis, and thermal evaporation are 30.0%,[32] 80.0%,[42] and 82.0%,[43] respectively. The mass of direct emissions are determined as the mass of the cleaning solvents of ethanol and deionized water, and waste silver paste, BL-TiO_2 ink, nc-TiO_2 ink, PbI_2, and spiro-OMeTAD materials. Due to the lack of life cycle impact assessment results for several important components of the perovskite solar modules, we further establish the material inventories of PbI_2, CH_3NH_3I, spiro-OMeTAD, FTO glass, ITO glass, BL-TiO_2 ink, nc-TiO_2 ink, ZnO ink, and silver paste. The detailed manufacturing routes, inventory tables, and life cycle impact assessment results are given in the Supplementary Information.

Table 2 Material inventory of 1 m^2 of the TiO_2 module with a 70.0% active area

	Mass (kg)	Note
Raw materials		
Substrate patterning		
FTO glass	5.04	Substrate
Ethanol	2.58×10^{-2}	Substrate cleaning solvent

Deionized water	3.27×10^{-2}	Substrate cleaning solvent
Silver paste	8.81×10^{-3}	Metallic mask
Hydrogen chloride solution	6.95×10^{-3}	Metallic mask cleaning solvent
Blocking layer deposition		
BL-TiO_2 ink	1.83×10^{-2}	Layer thickness 100 nm
Ethanol	2.58×10^{-2}	Substrate cleaning solvent
Deionized water	3.27×10^{-2}	Substrate cleaning solvent
Electron-transport layer deposition		
nc-TiO_2 ink	4.94×10^{-3}	Layer thickness 250 nm
Perovskite layer deposition		
PbI_2	1.38×10^{-3}	Layer thickness 96 nm
Dimethylformamide	2.83×10^{-3}	Solvent of PbI_2
CH_3NH_3I	1.43×10^{-4}	Layer thickness 204 nm
Isopropanol	1.12×10^{-2}	Solvent of CH_3NH_3I
Hole-transport layer deposition		
Spiro-OMeTAD	8.50×10^{-4}	Layer thickness 200 nm
Chlorobenzene	1.18×10^{-2}	Solvent of spiro-OMeTAD
Cathode deposition		
Au	1.65×10^{-3}	Layer thickness 100 nm
Encapsulation[a]		
Adhesive	2.02×10^{-2}	3 M 467 MPF
PET	6.17×10^{-2}	Applied on 2 sides
Direct emissions		
Ethanol	6.81×10^{-2}	Substrate cleaning solvent
Silver	6.17×10^{-3}	Silver paste
Butyl acetate	2.64×10^{-3}	Silver paste thinner
Hydrogen chloride solution	2.08×10^{-3}	Metallic mask cleaning solvent
Titanium tetrachloride	1.76×10^{-4}	Wasted concentrate of BL-TiO_2 ink
Isopropanol	1.23×10^{-2}	Solvent of BL-TiO_2 ink and CH_3NH_3I
Acetone	5.38×10^{-4}	Solvent of BL-TiO_2 ink
Acetic anhydride	9.46×10^{-4}	Solvent of BL-TiO_2 ink
Terpineol	4.20×10^{-3}	Solvent of nc-TiO_2 ink
PbI_2	9.66×10^{-4}	Wasted PbI_2
Dimethylformamide	2.83×10^{-3}	Solvent of PbI_2
Spiro-OMeTAD	5.95×10^{-4}	Wasted Spiro-OMeTAD
Chlorobenzene	1.18×10^{-2}	Solvent of spiro-OMeTAD
Gold	2.97×10^{-4}	Wasted cathode
Disposal materials	5.13	To landfill

a. the encapsulation parameters are reported by Espinosa *et al.*[34]

The energy inventory of 1 m^2 of the TiO_2 module is shown in Table 3. As can be seen, all the operations are performed using electric equipment. Therefore, energy consumption is evaluated by multiplying equipment power by corresponding operating time. Specifically, the powers for ultrasonic cleaning, screen printing, sintering, and spray pyrolysis are applied with that of typical commercially available equipment;[7, 44-47] the energy consumption for spin coating and thermal evaporation are obtained from Garcia-Valverde *et al.*[32] In terms of encapsulating the perovskite

solar module, we apply the same energy consumption as that evaluated by Espinosa *et al.*[34] The total electricity consumption for manufacturing 1 m^2 of the perovskite solar module is 7.78 kWh.

Table 3 Energy consumption for manufacturing 1 m^2 of the TiO_2 module with a 70.0% active area

	Power (W)	Time (s)	Electricity (MJ)
Substrate patterning			
Ultrasonic cleaning[45]	1.45×10^{3}	1.20×10^{3}	1.74
Screen printing[47]	6.42×10^{3}	6.00	3.85×10^{-2}
Sintering[44]	3.05×10^{3}	1.80×10^{3}	5.50
Blocking layer deposition			
Spray pyrolysis[46]	1.30×10^{2}	2.65×10	3.44×10^{-3}
Electron-transport layer deposition			
Screen printing[47]	6.42×10^{3}	6.00	3.85×10^{-2}
Sintering[44]	3.27×10^{3}	1.80×10^{3}	5.88
Perovskite layer deposition			
PbI_2 spin coating[32]	2.02×10^{4}	4.00×10	8.08×10^{-1}
Sintering[44]	3.55×10^{2}	3.60×10^{3}	1.28
Hole-transport layer deposition			
Spiro-OMeTAD spin coating[32]	2.69×10^{4}	3.00×10	8.08×10^{-1}
Cathode evaporation[32]			1.19×10
Encapsulation[34]			1.48×10^{-2}
Total			7.78 (kWh)

Table 4 and Table 5 summarize the material and energy inventory of 1 m^2 of the ZnO module, respectively. The mass of ITO glass is evaluated from the data reported in the literature.[32] The LCI and impact assessment results of ITO glass and ZnO ink are given in the Supplementary Information.

Table 4 Material inventory of 1 m^2 of the ZnO module with a 70.0% active area

	Mass (kg)	Note
Raw materials		
Substrate patterning		
ITO glass	1.54	Substrate
Ethanol	2.58×10^{-2}	Substrate cleaning solvent
Deionized water	3.27×10^{-2}	Substrate cleaning solvent
Electron-transport layer deposition		
ZnO ink	4.59×10^{-2}	Layer thickness 25 nm
Perovskite layer deposition		
PbI_2	1.38×10^{-3}	Layer thickness 96 nm
Dimethylformamide	2.83×10^{-3}	Solvent of PbI_2
CH_3NH_3I	1.40×10^{-4}	Layer thickness 204 nm
Isopropanol	1.12×10^{-2}	Solvent of CH_3NH_3I
Hole-transport layer deposition		
Spiro-OMeTAD	8.50×10^{-4}	Layer thickness 200 nm

Chlorobenzene	1.18×10^{-2}	Solvent of spiro-OMeTAD
Cathode deposition		
Ag	1.19×10^{-3}	Layer thickness 150 nm
Encapsulation[a]		
Adhesive	2.02×10^{-2}	3 M 467 MPF
PET	6.17×10^{-2}	Applied on 2 sides
Direct emissions		
Ethanol	2.58×10^{-2}	Substrate cleaning solvent
Zinc acetate dihydrate	6.17×10^{-4}	Wasted concentrate in ZnO ink
Potassium hydroxide	4.43×10^{-4}	Solvent of ZnO ink
n-Butanol	3.80×10^{-2}	Solvent of ZnO ink
Methanol	5.71×10^{-2}	Solvent of ZnO ink
Chloroform	4.96×10^{-3}	Solvent of ZnO ink
PbI_2	9.66×10^{-4}	Wasted PbI_2
Dimethylformamide	2.83×10^{-3}	Solvent of PbI_2
Isopropanol	1.12×10^{-2}	Solvent of CH_3NH_3I
Spiro-OMeTAD	5.95×10^{-4}	Wasted Spiro-OMeTAD
Chlorobenzene	1.18×10^{-2}	Solvent of spiro-OMeTAD
Silver	2.15×10^{-4}	Wasted cathode
Disposal materials	1.63	To landfill

a. the encapsulation parameters are reported by Espinosa *et al.*[34]

Table 5 Energy consumption for manufacturing 1 m^2 of the ZnO module with a 70.0% active area

	Power (W)	Time (s)	Electricity (MJ)
Substrate patterning			
Ultrasonic cleaning[45]	1.45×10^{3}	1.20×10^{3}	1.74
Electron-transport layer deposition			
ZnO spin coating[32]	2.02×10^{4}	9.00×10	1.82
Perovskite layer deposition			
PbI_2 spin coating[32]	2.02×10^{4}	1.50×10	3.03×10^{-1}
Hole-transport layer deposition			
Spiro-OMeTAD spin coating[32]	2.69×10^{4}	3.00×10	8.08×10^{-1}
Cathode evaporation[32]			1.17×10
Encapsulation[34]			1.48×10^{-2}
Total			4.56 (kWh)

2.3.Life cycle impact assessment

In the impact assessment phase, the LCI data are converted to various indicators, which provide the basis for analyzing the contributions of individual entries in the inventory to a number of environmental impacts. In the current study, we focus on 16 midpoint indicators according to the CML method,[48] cumulative energy consumption,[40] and Intergovernmental Panel on Climate Change (IPCC) 2013 (climate change) method,[49] and three endpoint indicators following the Eco-indicator 99 methodology.[50] We also evaluate two important indicators: EPBT and CO_2 emission

factor, which are widely used for PV technology LCA. The characterization factors for all materials are also explicitly shown in the Supplementary Information.

In the CML method,[48] a set of impact categories and characterization methods are introduced to evaluate the environment profile of a product. We investigate 14 impact categories in the CML method, namely acidification, eutrophication, fresh water aquatic ecotoxicity, fresh water sediment ecotoxicity, human toxicity, ionizing radiation, land use, malodours air, marine aquatic ecotoxicity, marine sediment ecotoxicity, photochemical oxidation, depletion of abiotic resources, stratospheric ozone depletion, and terrestrial ecotoxicity.

Primary energy refers to the energy extracted from nature that has not been transformed to any forms of secondary energy, like electricity, gasoline, *etc*. Examples of primary energy include fossil fuels, nuclear energy, solar energy, wind energy, geothermal energy, and biomass. The primary energy consumption, or cumulative energy consumption of a PV device sums up various types of primary energy as suggested by many PV LCA practitioners.[34, 51-53] Specifically in Ecoinvent, we sum up the entries in cumulative energy demand to obtain the primary energy consumption of manufacturing a material, including biomass, fossil, geothermal, nuclear, primary forest, solar, water, and wind. For a perovskite module, the primary energy consumption comes from the energy embedded in the raw materials, the energy consumed in manufacturing, and the energy consumed in the end-of-life phase. The embedded primary energy is retrieved from Ecoinvent if the material is available in the database. Otherwise, for nine important components of the perovskite PV modules, we develop their manufacturing routes and estimate the embedded primary energy in the Supplementary Information. We translate heat and electricity consumption in manufacturing to equivalent primary energy consumption assuming that heat is supplied by a natural-gas plant, and electricity use applies the average electricity mix in the US.[40] The conversion coefficients for heat and electricity are 1.17 MJ primary energy/MJ heat and 12.7 MJ primary energy/kWh, respectively. The end-of-life primary energy consumption accounts for the energy usage involved in landfilling the waste modules.

Carbon footprint is another prevalent impact indicator in the LCA of PV technologies.[26, 28, 34, 36] As a relative measurement, carbon footprint quantifies the total greenhouse effect of a material based on the global warming potentials of GHGs published by IPCC.[49] Similar to primary energy consumption, the carbon footprint of a perovskite module is contributed by raw materials, energy consumption and direct emissions during manufacturing and landfilling.

The above indicators are derived from midpoints methods, which directly applies characterization factors to LCI results. In contrast, Eco-indicator 99 is an endpoint methodology, which allocates the midpoint categories to three damage categories: ecosystem quality, human health, and resources.[50] There are three perspectives available in Eco-indicator 99: Egalitarian, Hierarchist, and Individualist, varying by the timeframe, manageability, and evidence.[54] We choose the Egalitarian perspective corresponding to the (E, E) results in Ecoinvent, following the same selection by Espinosa *et al*.[34]

The life cycle impact assessment results are further employed to generate two sustainability indicators: EPBT and CO_2 emission factor. In our analysis, the EPBT of a perovskite solar module is defined as the ratio between the total primary energy consumption and the annual electricity generation. The latter depends on the annual insolation of an area, and the module efficiency and performance ratio of a PV system. The values of these parameters are given in the "Mean" column of Table 6. Note that when we compare the performance among various PV technologies, uniform values of insolation (1.70×10^3 kWh/m^2/year) and performance ratio (75.0%) representing a typical Southern European condition are applied. Relatively high values (1.96×10^3 kWh/m^2/year and 80.0%) for the San Francisco area in the US are selected in the uncertainty analysis and sensitivity analysis in order to reduce the uncertainty caused by geographical discrepancy, and also to explore the potential performance of this emerging PV technology in a popular solar market.[38]

Table 6. Summary of uncertain parameters[38, 39]

	Mean	Geometric standard deviation	Pedigree matrix
Normal distribution			
Insolation (kWh/m^2/year)	1.96×10^3	5.89×10	
Lognormal distribution			
TiO_2 Carbon foot print (g CO_2-eq/m^2)	2.17×10	1.11	(4, 4, 1, 1, 1, 2)
TiO_2 primary energy consumption (MJ/m^2)	4.46×10^2	1.11	(4, 4, 1, 1, 1, 2)
TiO_2 Module efficiency	9.10%	1.05	(1, 4, 1, 1, 1, 2)
ZnO Carbon foot print (g CO_2-eq/m^2)	1.91×10	1.11	(4, 4, 1, 1, 1, 2)
ZnO primary energy consumption (MJ/m^2)	3.92×10^2	1.11	(4, 4, 1, 1, 1, 2)
ZnO Module efficiency	11.0%	1.05	(1, 4, 1, 1, 1, 2)
Performance ratio	80.0%	1.23	(3, 1, 5, 1, 1, 1)
Lifetime (year)	2.00	1.15	(5, 4, 1, 1, 1, 5)

In addition to EPBT, CO_2 emission factor is another important sustainability indicator of PV modules. The CO_2 emission factor of a PV module can be obtained if the carbon footprint is

divided by the electricity generated during the entire life cycle. Thus, we need to know the lifetime of the PV system in addition to the parameters for calculating the annual electricity generation. Limited by the fact that perovskite PVs are still at an early development stage, no exact lifetime for a perovskite solar module has been announced yet. As reported by Liu and coworkers,[55] a compact-layer-free planar perovskite solar cell sustains relative cell efficiencies greater than 20% for up to 60 hours. Another hole-conductor-free mesoscopic perovskite solar cell can however be stable for over a month in an ambient environment under illumination.[56] There is no doubt that the encapsulation for a solar module is able to prolong the lifetime of a PV module well beyond a month.[57] According to Kamat,[58] the simplicity of the fabrication and relatively high power conversion efficiencies offer perovskite PVs advantages over traditional thin-film PVs, which have been proven with lifetime of tens of years.[59] Therefore, we make a conservative assumption that the perovskite modules are able to operate for 2 years based on the "approaching 3-year lifetime" of organic PVs.[60, 61]

It is reasonable to assume that reliable results of EPBT and CO_2 emission factor are dependent on accurate input parameters. However, it is not uncommon that fluctuation occurs in the primary energy consumption and carbon footprint results due to the fact that these results are based on stoichiometric relationships; a precise estimation of lifetime for perovskite PVs still is a difficult task at the current stage; several parameters, such as power conversion efficiencies, insolation, and performance ratios, exhibit inherent uncertainties regardless of the readiness level of the PV technology.[38] Therefore, probability distributions are applied to the key input parameters based on literature data and a pedigree method,[62] and simulation methods are further used to investigate the influence of uncertain parameters on sustainability indicators introduced above. As shown in Table 6, insolation is assigned with a normal distribution, whose coefficients follow the same assumptions made by Yue et al.[38] In contrast, the other eight parameters are assigned with lognormal distributions, whose geometric standard deviations are estimated following the pedigree-matrix based approach introduced by Ecoinvent.[62] The pedigree matrices in our estimation are given in Table 6. The simulation is accomplished with Oracle Crystal Ball,[63] which takes advantage of the Monte Carlo simulation method in uncertainty analysis. In addition to the distribution assumptions, we define four forecasts in the Monte Carlo simulations for EPBT and CO_2 emission factor with respect to two solar modules, and the number of trials is set as 100,000. Based on the simulation results, we further conduct sensitivity analyses for the four forecasts and

identify the most influential parameters for the development of sustainable perovskite solar modules.

2.4.Life cycle interpretation

The LCI of the two perovskite solar modules contain important information about the distributions of materials and resources consumed, which builds the foundation of the distributions of environmental impacts. A simple observation shows the dominant mass of the substrates for both modules and intensive energy consumption during thermal evaporation. In life cycle impact assessment, we identify the significant factors and provide guidance to the improvement of sustainability of the two perovskite solar modules through comprehensively comparing their life cycle impact indicators, Eco-indicator 99 results, as well as EPBTs and CO_2 emission factors. More insightful suggestions are given following uncertainty analysis and sensitivity analysis.

3. Results and discussions

3.1.Primary energy consumption and carbon footprint

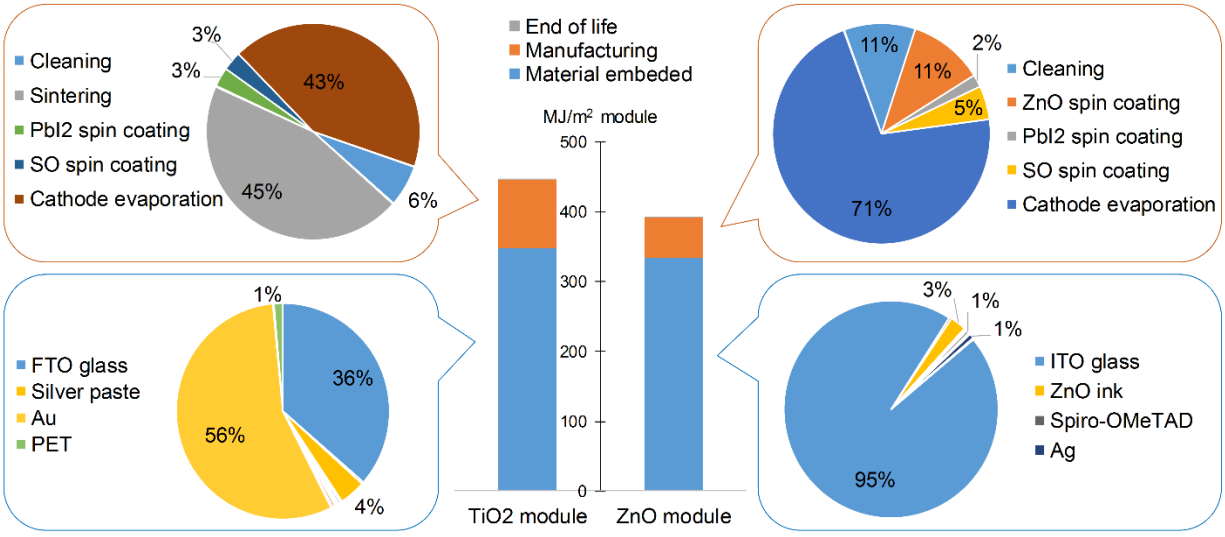

Figure 3. Distributions of the primary energy consumption for manufacturing two perovskite solar modules. Contributions less than 1% are not shown in the pie charts.

The impact categories paid the tremendous attention to in the PV LCA studies are primary energy consumption and carbon footprint. Based on the LCI derived in the last section, the primary

energy consumption and carbon footprint and their distributions for both perovskite modules are calculated and illustrated in Figure 3 and Figure 4, respectively.

As can be seen in Figure 3, raw materials contribute to about 80% primary energy consumption in both modules. However, the breakdown of the materials embedded energy reveals differences between the perovskite modules. FTO glass and gold cathode are the major contributors to the embedded primary energy of the TiO_2 module, while ITO glass is the only outweighing component in the ZnO module. It is not surprising that the substrates are the most influential component in both modules, because they dominate the total mass of the modules (98% for the TiO_2 module and 95% for the ZnO module). The reason for a 36% share residing in gold cathode for the TiO_2 module is because gold is a precious metal with considerably high primary energy consumption and embedded GHG emissions.[40] Although a small amount of gold is used as the cathode, the embedded primary energy of this layer is still significant. In contrast, the ZnO module employs silver as the cathode, resulting in a much smaller primary energy consumption. Nevertheless, we also notice that the ITO substrate consumes about 2.5 times the primary energy embedded in the FTO substrates. Similar to the case of gold, the use of energy-intensive indium is responsible for the unfavorable environmental performance of ITO substrates. Future effort should be spent on identifying suitable replacement materials for gold cathode in the TiO_2 module, and ITO glass in the ZnO module.

With respect to the primary energy consumed in manufacturing, long-time and high-temperature sintering results in the highest electricity demand in the TiO_2 module. Additionally, cathode evaporation consume 43% of the electricity in the TiO_2 module manufacturing, and 71% in the ZnO module manufacturing. The thermal evaporation is accomplished by heating solid metal to vapor particles in vacuum and condensing back to solid on the substrate surface. This technology deposits a thin film of metal with high quality, but at a high energy cost.[64, 65] Therefore, replacement of sintering and thermal evaporation with alternative deposition techniques can potentially reduce the primary energy consumption.

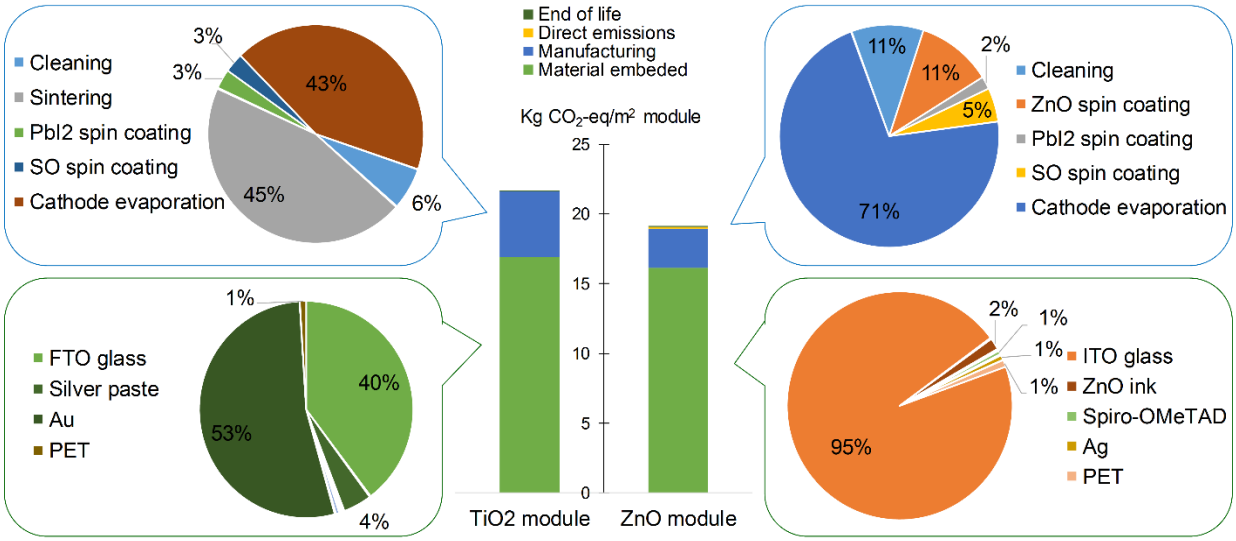

Figure 4. Distributions of the carbon footprint of two perovskite solar modules. Contributions less than 1% are not shown in the pie charts.

We show the distribution of carbon footprint in Figure 4, from which the major contributors of substrate, gold cathode, thermal evaporation, and sintering can be identified. Same manufacturing distributions can be found in the results of primary energy consumption and carbon footprint, because different manufacturing operations consume only electricity and apply the same set of characterization factors in the evaluation. Not only are the distributions of primary energy consumption and carbon footprint the same, but the distributions of other impact categories are also identical as long as the manufacturing procedure is not changed. A resemblance can be found between the distributions of the material embedded primary energy consumption and carbon footprint, which suggest similar strategies for more environmental sustainable modules.

3.2.Environmental profiles for the life cycle of two perovskite modules

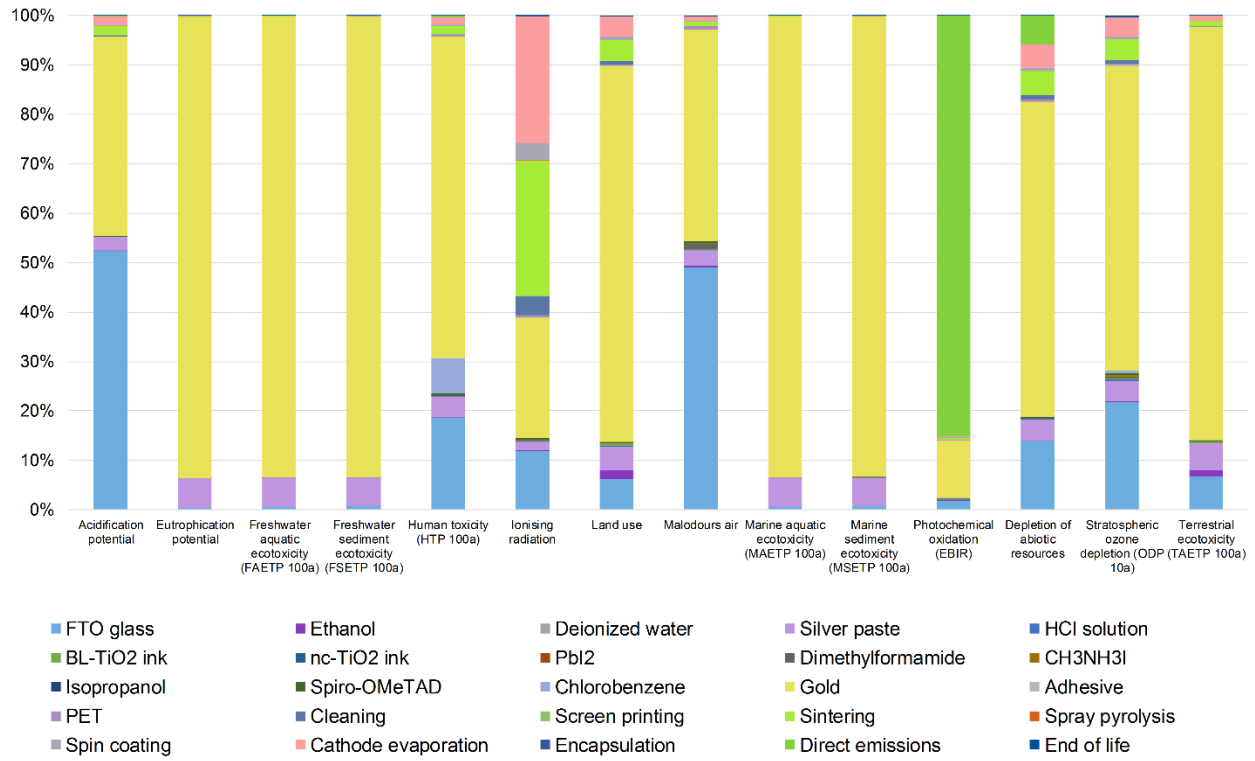

Figure 5. Environmental profile of 1 m^2 of the TiO_2 module.

Figure 5 and Figure 6 shows the environmental profiles of 1 m^2 of the TiO_2 module and 1 m^2 of the ZnO module, respectively. All 14 impact indicators are normalized, so that the total indicator of each impact category is 100%. In Figure 5, gold cathode is the most significant contributor to eutrophication (93%), fresh water aquatic ecotoxicity (93%), fresh water sediment ecotoxicity (93%), human toxicity (65%), land use (76%), marine aquatic ecotoxicity (93%), marine sediment ecotoxicity (93%), depletion of abiotic resources (64%), stratospheric ozone depletion (62%), and terrestrial ecotoxicity (84%). Gold also has great influence on acidification (40%) and malodours air (43%). The reason is similar to the dominant contribution of gold in both primary energy consumption and carbon footprint of the TiO_2 module. The production of gold from ores not only requires a large amount of energy, but also leads to the release of toxic mine drainage into lakes and rivers. The drainage contains nitrates, sulfides, arsenic, antimony, and mercury, which can cause acidification and eutrophication, and are extremely harmful to aquatic organisms.[66] Therefore, the use of gold is environmentally expensive, and the replacement of gold results in a substantial reduction in most environment impacts.

In addition to the use of gold, FTO glass contributes to 52% in acidification, and 49% in malodours air. This is because the production of FTO glass generates massive direct air emissions, including carbon dioxide, nitrogen oxide, and sulfur oxide, which are easy to react with water and form acid in ocean and freshwater, or cause severe air pollution in the atmosphere. Moreover, the direct emissions during manufacturing contributes to 85% in photochemical oxidation. Photochemical oxidation, or alternatively known as summer smog, is formed in the condition of sunlight, nitrogen oxide, and organic emissions. The direct emissions in manufacturing are primarily organic solvents that are emitted to the atmosphere during drying. In future designs, recycling organic solvents, such as ethanol, acetone, isopropanol, and chlorobenzene, can drastically reduce the photochemical oxidation effect caused by manufacturing perovskite solar modules.

As shown in Figure 6 for the ZnO module, the silver cathode is an influential contributor, but not as significant as the gold in the TiO_2 module. Silver is responsible for 40% in eutrophication, 52% in fresh water aquatic ecotoxicity, 50% in fresh water sediment ecotoxicity, 51% in marine aquatic ecotoxicity, and 49% in marine sediment ecotoxicity. Although gold is always coproduced with silver, the presence of silver in other ores (such as silver-lead-zinc ore) and the lower price on the market allow silver to bear much smaller environmental burdens than gold. Among several available cathode materials, silver is favorable in terms of both conducting performance and environmental impacts.[23] In contrast, ITO glass dominates the impact categories of acidification, eutrophication, human toxicity, ionizing radiation, land use, malodours air, depletion of abiotic resources, and terrestrial ecotoxicity. This results from its vast energy consumption during manufacturing, the use of precious metal (such as indium), and the overwhelming mass ratio of the ITO glass over the module (95%). Regarding the overall environmental performance, ITO glass is not a good option compared with FTO glass. It is also worth noticing that ZnO ink is responsible for 85% of the stratospheric ozone depletion impact, which is the result of applying chloroform as part of the solvent. Chloroform is among the chemicals that are able to convert ozone to oxygen. In order to develop a perovskite module with lower ozone depletion potential, it is better to choose alternative organic solvents to chloroform.

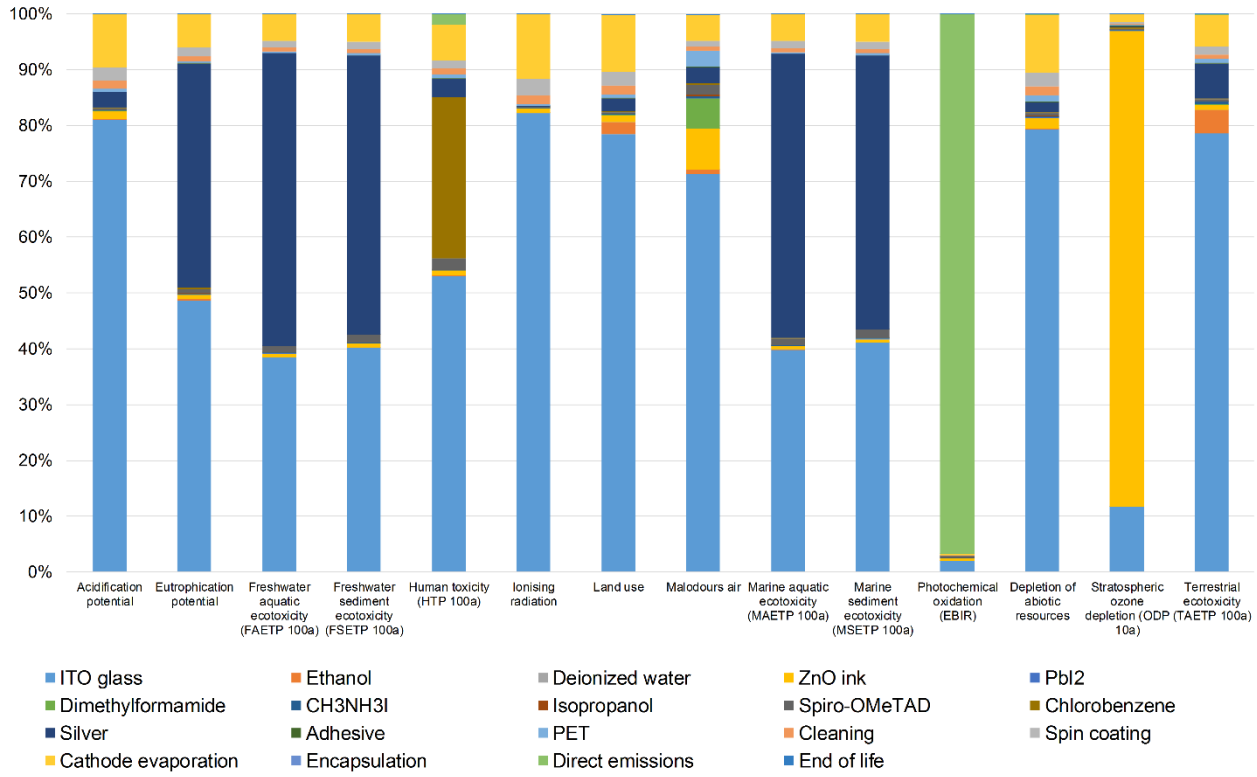

Figure 6. Environmental profile of 1 m^2 of the ZnO module.

We compare the life cycle impact assessment results between the two modules in Figure 7. The TiO_2 module is used as the standard for normalization. It can be seen that the ZnO module performs in a more environmentally friendly manner except three impact categories: ionizing radiation, photochemical oxidation, and stratospheric ozone depletion. Although the ionizing radiation of the ZnO module is about twice that of TiO2 module, the absolute indicator values of both modules are not considered harmful.

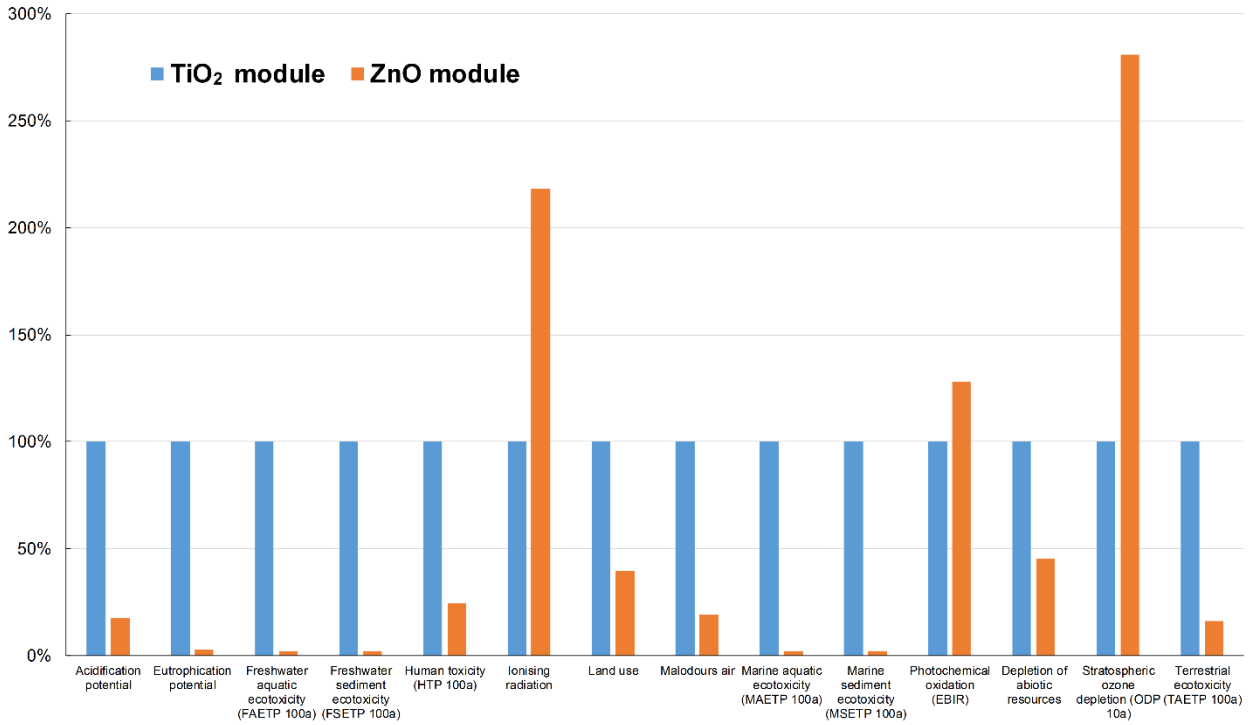

Figure 7. Life cycle impact assessment comparison between 1 m^2 of the TiO_2 module and 1 m^2 of the ZnO module.

We compare the Eco-indicator 99 results for eight PV modules in Figure 8. In all three damage categories, namely ecosystem quality, human health, and resources, the ZnO module achieves the second lowest points. Even though higher than the results of OPV, the Eco-indicators 99 points of the ZnO module are one order of magnitude lower than the results of c-Si, a-Si, Ribbon-Si, CdTe, CIS, and the TiO_2 module. This clearly demonstrates the overall environmental advantage of the ZnO module. Contrarily, the TiO_2 module has the highest total points, as a result of using the environmentally expensive gold as the cathode metal. Therefore, a more environmentally

sustainable perovskite module can be developed based on the ZnO module, through switching to greener substrates and reducing the consumption of organic solvents.

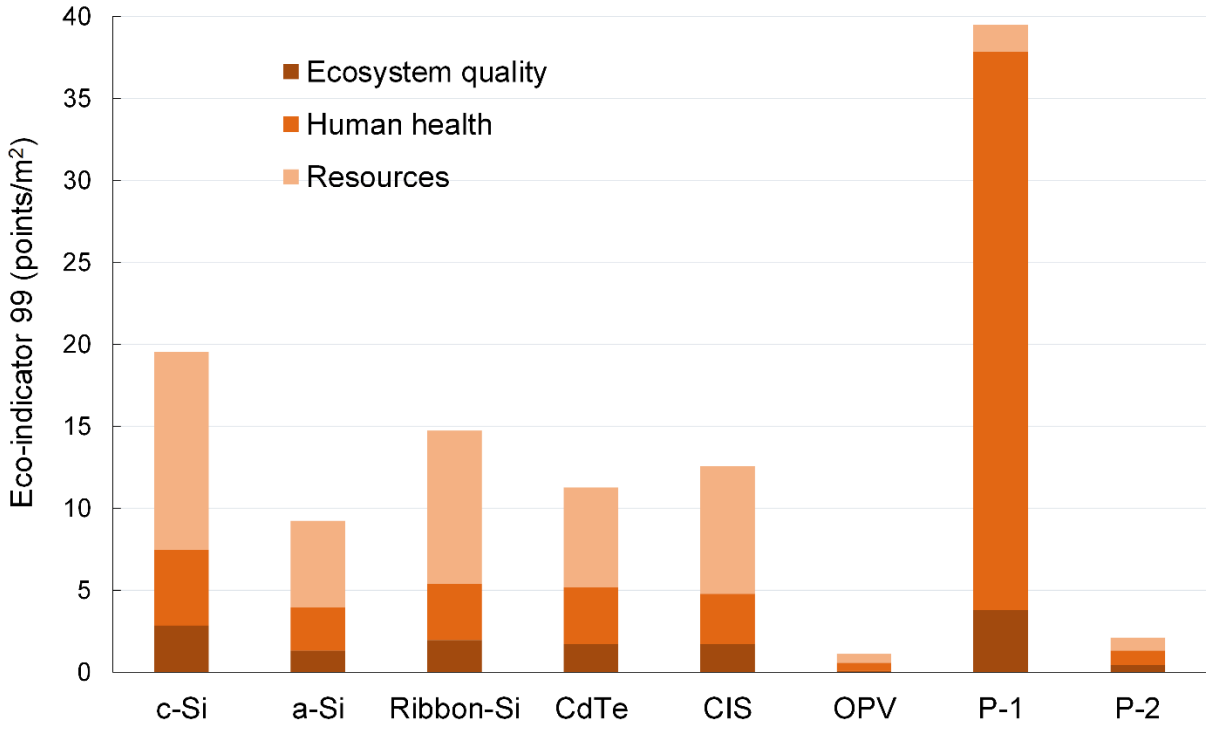

Figure 8. Eco-indicator 99 results for 1 m2 of eight PV modules. P-1 represents the TiO_2 perovskite module; P-2 represents the ZnO perovskite module. The data for c-Si, a-Si, Ribbon-Si, CdTe, and CIS are extracted from Laleman *et al*.[54] The data for OPV are extracted from Espinosa *et al*.[34]

3.3. Comparison with existing PV technologies

The EPBT comparison among seven PV modules are shown in Figure 9. Based on the carbon footprint, primary energy consumption, and module efficiency distributions in Table 6, we calculate the 95% confident regions for the two perovskite PVs and show the error bars in Figure 9. Uncertain EPBT regions for other PV technologies are not reported, but it is expected that more mature technologies have smaller error bars. It can be seen that perovskite has shorter nominal EPBT than the other technologies. The ZnO perovskite module achieves the shortest nominal EPBT of 0.22 years. The reason for perovskite modules outperforming silicon-based modules and CdTe modules lies in the avoidance of using high-purity silicon or rare metals that embed

considerably high environmental burdens. The OPV module has a slightly longer EPBT. The favorable performance against silicon-based modules and CdTe modules is largely accredited to the recent development of a roll-to-roll process.[23, 67] The EPBT of a perovskite module can be aggressively reduced in the future with more efficient processing technologies.

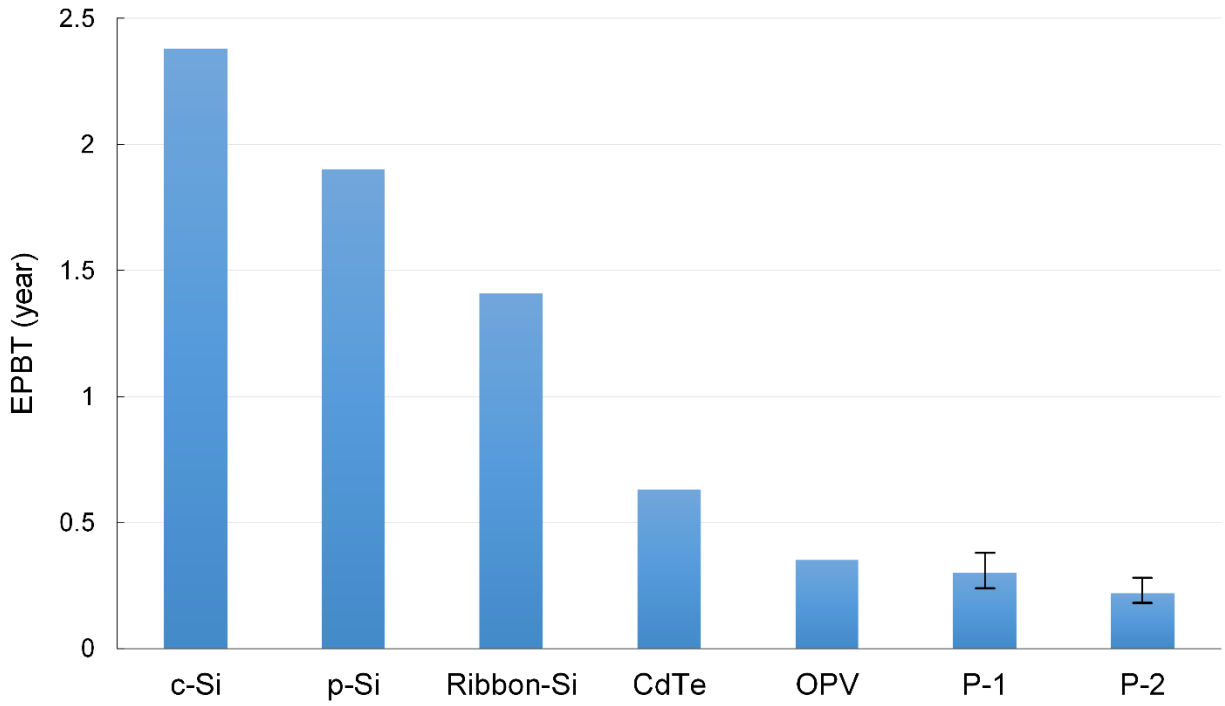

Figure 9. Energy payback time for seven PV modules. P-1 represents the TiO_2 perovskite module; P-2 represents the ZnO perovskite module. The estimations are based on rooftop-mounted installation, Southern European insolation, 1.70×10^3 kWh/m^2/year, and a performance ratio of 0.750. The data for c-Si, p-Si, Ribbon-Si, CdTe, and OPV are extracted from Darling *et al*.[36] The error bars of P-1 and P-2 represent 95% confident regions.

Figure 10 shows the CO_2 emission factors for seven PV technologies. Error bars of the two perovskite solar modules are calculated considering the carbon footprint, primary energy consumption, module efficiency, and lifetime distributions in Table 6. Uncertain CO_2 emission factors for other PV technologies are not reported, but it is expected that more mature technologies have smaller error bars. Perovskite solar modules, however, show relatively large CO_2 emission

factors in both types of modules, which means the "CO_2 price" of the perovskite solar modules is still high at the current stage. It is noted that as a relatively new technology, OPVs also suffer from a large CO_2 emission factor. This result is mainly because of the short lifetime of the modules, which is assumed as only 2 years, as opposed to more than 20 years for silicon-based modules. It is highly likely that the lifetime of perovskite PVs will increase substantially with advancement in materials and design, which means that perovskite PV has the potential for a far lower CO_2 emission factor in the future.

These results deliver an important message for the development of perovskite solar cells, namely, that perovskites are potentially the most environmentally sustainable PV option to date. Perovskite technology is the youngest among the PV technologies, and it possesses the potential for better manufacturing processes with even higher efficiency, more stable performance and longer operation lifetime.

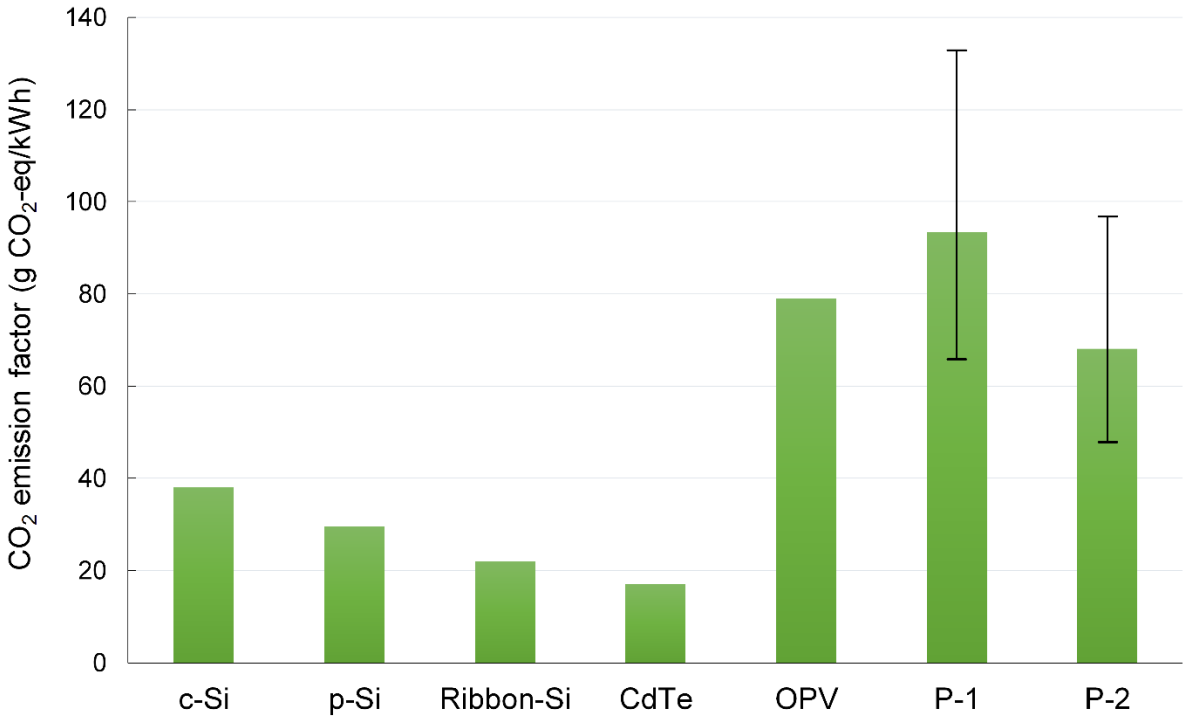

Figure 10. CO_2 emission factor for seven PV modules. P-1 represents the TiO_2 perovskite module; P-2 represents the TiO_2 perovskite module. The estimations are based on rooftop-mounted installation, Southern European insolation, 1.70×10^3 kWh/m^2/year, and a performance ratio of 0.750. The data for c-Si,

p-Si, Ribbon-Si, CdTe, and OPV are extracted from Darling *et al.*[36] The error bars of P-1 and P-2 represent 95% confident regions.

3.4. Uncertainty analysis and sensitivity analysis

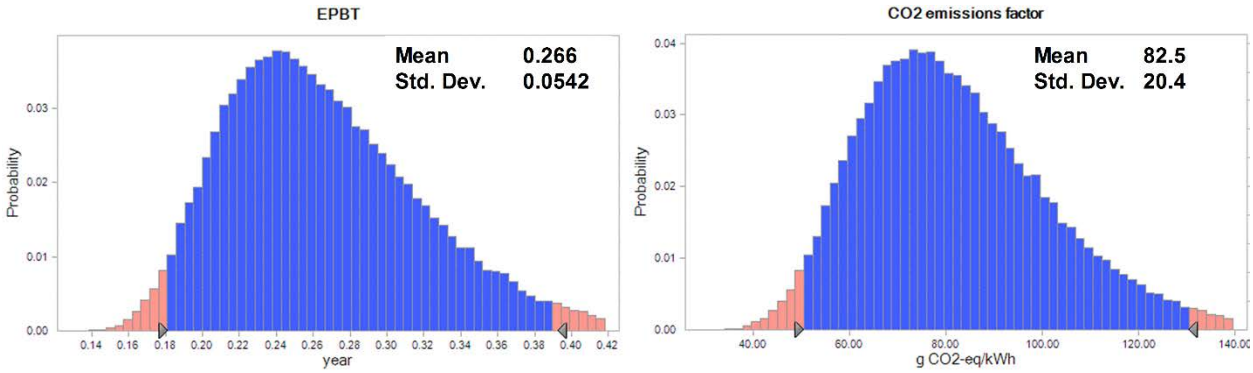

Figure 11 Probability distributions for energy payback time (EPBT) and CO_2 emission factor of the TiO_2 Module.

The probability distributions of the two forecasts for the TiO_2 module are shown in Figure 11. Both distributions demonstrate a wide range, with the highest bars representing the values of the highest probabilities. The asymmetric profile of both distributions results from the nonlinear relationship between the input parameters and the sustainability indicators.

Table 7. Simulation results for two perovskite modules.

Module		TiO_2	ZnO
EPBT (year)	Mean	0.266	0.193
	Standard deviation	0.0542	0.0392
	95% confident region	(0.182, 0.391)	(0.132, 0.283)
CO_2 emission factor (g CO_2-eq/kWh)	Mean	82.5	60.1
	Standard deviation	20.4	14.8
	95% confident region	(50.7, 130)	(37.0, 94.5)

The simulation results are summarized in Table 7. It can be seen that EPBT's in both cases are comparatively robust when the key specifications of the module are subject to uncertainty. The low EPBT's for the entire 95% confident regions demonstrate that perovskite is already considerably competitive in terms of energy recovery. However, from both Figure 11 and Table 7,

the CO_2 emission factors are found unstable in the presence of parameter uncertainties, and the values are much higher than those of the other technologies. Therefore, the next step toward more environmentally sustainable perovskite PVs could be to apply simple and scalable manufacturing methods with less GHG emissions. Promising methods include using slot die coating instead of spin coating, and screen printing instead of thermal evaporation.[23]

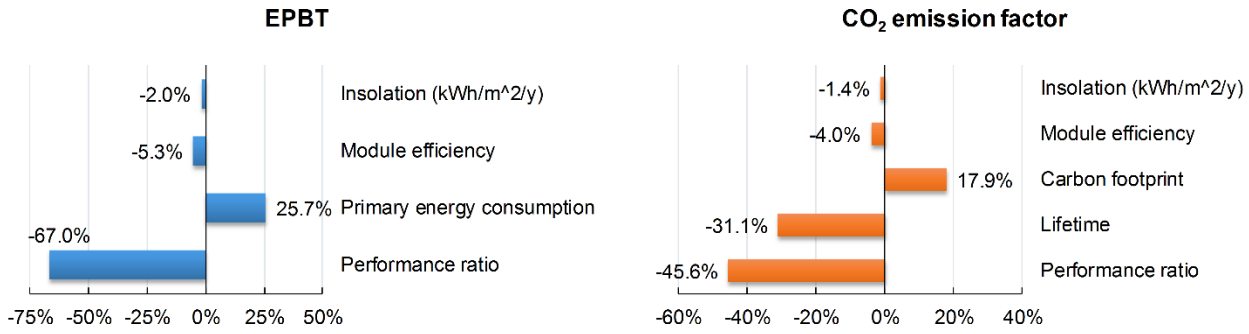

Figure 12. Sensitivity analysis for energy payback time (EPBT) and CO_2 emission factor of the TiO_2 Module.

Next, we conduct sensitivity analyses for EPBT and CO_2 emission factor with respect to two solar modules. Due to the similarity between the results, the uncertainty and sensitivity analysis for the ZnO module are presented in the Supplementary Information. Since the EPBT is much shorter than one year, the influence of lifetime on EPBT are negligible. In contrast, the fluctuations in performance ratio, primary energy consumption, module efficiency, and insolation are responsible for the deviation of EPBT from its nominal value. In Figure 12, the minus sign means that increasing these parameters causes EPBT to decline. Performance ratio shows the most significant influence and contributes to 67.0% of the variance, while isolation accounts for only 2.0% of the variance. In the sensitivity results for CO_2 emission factor, it is noted that performance ratio is still the major contributor (45.6%). This parameter can be improved with better inverter equipment, effective surface protection layer, and efficient system arrangement, as well as efforts in the power transmission system. It deserves our attention that lifetime also significantly impacts CO_2 emission factor (31.1%), emphasizing the role of device stability in order to develop more environmentally sustainable perovskite solar modules with ultimately low CO_2 prices.

From the above results, perovskite PV modules demonstrate robust environmental behavior with respect to EPBT. We identify performance ratio and lifetime as the influential input

parameters in order to effectively improve the sustainability of a perovskite PV module. With an ambitious leap to over 20% module efficiency in a durable device, perovskite PVs would surely be positioned to become a major player in the energy sector.[3]

4. Conclusion

With continuous record-breaking power conversion efficiencies reported in the past few years, perovskite PVs must now be considered a potential serious challenger to other PV technologies for electricity generation. Despite their development being at an early stage, perovskite PVs have shown excellent potential for environmental sustainability. In this work, we perform a cradle-to-grave life cycle assessment of two solution-processed perovskite solar modules based on the manufacturing procedures described by Matteocci *et al.*[10] and Liu *et al.*[6] The life cycle environmental impact assessment involves 16 midpoint impact categories, and an endpoint evaluation following the Eco-indicator 99 methodology. We shed light on two important sustainability indicators and find perovskite solar modules have the shortest EPBT among existing PV technologies. We find the environmental hotspots comes from the use of gold, ITO glass, and organic solvents, as well as energy intensive thermal evaporation. Moreover, we evaluate the sustainable indicators considering the uncertainties of major input parameters. The resulting probability distributions demonstrate that for perovskite PV at the current stage, EPBTs are stable and competitive, while CO_2 emission factors are less stable and comparatively sensitive to fluctuations. Lastly, through sensitivity analysis, we find that perovskite solar modules are potentially the most environmentally sustainable PV if future development confirms a larger performance ratio and a longer lifetime.

5. Acknowledgement

We gratefully acknowledge the financial support from the Institute for Sustainability and Energy at Northwestern University (ISEN). This work was performed, in part, at the Center for Nanoscale Materials, a U.S. Department of Energy, Office of Science, Office of Basic Energy Sciences User Facility under Contract no. DE-AC02-06CH11357. The authors thank C.-C. Ho for useful conversations regarding perovskite PV device processing.

References

1. U. S. EIA, *Annual energy outlook 2014*, Report DOE/EIA-0383(2014), Washington, DC, 2014.
2. H. J. Snaith, *J Phys Chem Lett*, 2013, 4, 3623-3630.
3. M. D. McGehee, *Nat Mater*, 2014, 13, 845-846.
4. R. F. Service, *Science*, 2014, 344, 458-458.
5. C. C. Stoumpos, C. D. Malliakas and M. G. Kanatzidis, *Inorg Chem*, 2013, 52, 9019-9038.
6. D. Y. Liu and T. L. Kelly, *Nat Photonics*, 2014, 8, 133-138.
7. H. P. Zhou, Q. Chen, G. Li, S. Luo, T. B. Song, H. S. Duan, Z. R. Hong, J. B. You, Y. S. Liu and Y. Yang, *Science*, 2014, 345, 542-546.
8. M. M. Lee, J. Teuscher, T. Miyasaka, T. N. Murakami and H. J. Snaith, *Science*, 2012, 338, 643-647.
9. A. Abrusci, S. D. Stranks, P. Docampo, H. L. Yip, A. K. Y. Jen and H. J. Snaith, *Nano Lett*, 2013, 13, 3124-3128.
10. F. Matteocci, L. Cinà, F. Di Giacomo, S. Razza, A. L. Palma, A. Guidobaldi, A. D'Epifanio, S. Licoccia, T. M. Brown, A. Reale and A. Di Carlo, *Progress in Photovoltaics: Research and Applications*, 2014, DOI: 10.1002/pip.2557, n/a-n/a.
11. J. M. Ball, M. M. Lee, A. Hey and H. J. Snaith, *Energ Environ Sci*, 2013, 6, 1739-1743.
12. H. S. Kim, C. R. Lee, J. H. Im, K. B. Lee, T. Moehl, A. Marchioro, S. J. Moon, R. Humphry-Baker, J. H. Yum, J. E. Moser, M. Gratzel and N. G. Park, *Sci Rep-Uk*, 2012, 2.
13. M. Z. Liu, M. B. Johnston and H. J. Snaith, *Nature*, 2013, 501, 395-398.
14. Q. Chen, H. P. Zhou, Z. R. Hong, S. Luo, H. S. Duan, H. H. Wang, Y. S. Liu, G. Li and Y. Yang, *J Am Chem Soc*, 2014, 136, 622-625.
15. P. W. Liang, C. Y. Liao, C. C. Chueh, F. Zuo, S. T. Williams, X. K. Xin, J. J. Lin and A. K. Y. Jen, *Adv Mater*, 2014, 26, 3748-3754.
16. J. Burschka, N. Pellet, S. J. Moon, R. Humphry-Baker, P. Gao, M. K. Nazeeruddin and M. Gratzel, *Nature*, 2013, 499, 316-+.
17. J. H. Heo, S. H. Im, J. H. Noh, T. N. Mandal, C.-S. Lim, J. A. Chang, Y. H. Lee, H.-j. Kim, A. Sarkar, K. NazeeruddinMd, M. Gratzel and S. I. Seok, *Nat Photon*, 2013, 7, 486-491.
18. D. Q. Bi, S. J. Moon, L. Haggman, G. Boschloo, L. Yang, E. M. J. Johansson, M. K. Nazeeruddin, M. Gratzel and A. Hagfeldt, *RSC Adv*, 2013, 3, 18762-18766.
19. G. Rebitzer, T. Ekvall, R. Frischknecht, D. Hunkeler, G. Norris, T. Rydberg, W. P. Schmidt, S. Suh, B. P. Weidema and D. W. Pennington, *Environ Int*, 2004, 30, 701-720.
20. K. Knapp and T. Jester, *Sol Energy*, 2001, 71, 165-172.
21. E. Alsema, *Renewable and Sustainable Energy Reviews*, 1998, 2, 387-415.
22. M. Raugei, S. Bargigli and S. Ulgiati, *Energy*, 2007, 32, 1310-1318.
23. N. Espinosa, R. Garcia-Valverde, A. Urbina and F. C. Krebs, *Sol Energ Mat Sol C*, 2011, 95, 1293-1302.
24. C. A. Wolden, J. Kurtin, J. B. Baxter, I. Repins, S. E. Shaheen, J. T. Torvik, A. A. Rockett, V. M. Fthenakis and E. S. Aydil, *Journal of Vacuum Science & Technology A*, 2011, 29, 030801.
25. E. A. Alsema and M. J. de Wild-Scholten, 2006.
26. V. M. Fthenakis and H. C. Kim, *Sol Energy*, 2011, 85, 1609-1628.
27. N. Jungbluth, *Prog Photovoltaics*, 2005, 13, 429-446.
28. H. Kim, K. Cha, V. M. Fthenakis, P. Sinha and T. Hur, *Sol Energy*, 2014, 103, 78-88.

29. S. Lizin, S. Van Passel, E. De Schepper, W. Maes, L. Lutsen, J. Manca and D. Vanderzande, *Energ Environ Sci*, 2013, 6, 3136-3149.
30. K. Kato, T. Hibino, K. Komoto, S. Ihara, S. Yamamoto and H. Fujihara, *Sol Energ Mat Sol C*, 2001, 67, 279-287.
31. V. M. Fthenakis, *Renewable and Sustainable Energy Reviews*, 2004, 8, 303-334.
32. R. Garcia-Valverde, J. A. Cherni and A. Urbina, *Prog Photovoltaics*, 2010, 18, 535-558.
33. N. Espinosa, R. Garcia-Valverde and F. C. Krebs, *Energ Environ Sci*, 2011, 4, 1547-1557.
34. N. Espinosa, M. Hosel, D. Angmo and F. C. Krebs, *Energ Environ Sci*, 2012, 5, 5117-5132.
35. A. L. Roes, E. A. Alsema, K. Blok and M. K. Patel, *Prog Photovoltaics*, 2009, 17, 372-393.
36. S. B. Darling and F. Q. You, *RSC Adv*, 2013, 3, 17633-17648.
37. D. J. Yue, F. Q. You and S. B. Darling, *Sol Energy*, 2014, 107, 380-380.
38. D. J. Yue, P. Khatav, F. Q. You and S. B. Darling, *Energ Environ Sci*, 2012, 5, 9163-9172.
39. S. B. Darling, F. Q. You, T. Veselka and A. Velosa, *Energ Environ Sci*, 2011, 4, 3133-3139.
40. Ecoinvent database v3.1, http://www.ecoinvent.ch/, Accessed December 2014.
41. U. Posset, M. Harsch, A. Rougier, B. Herbig, G. Schottner and G. Sextl, *RSC Adv*, 2012, 2, 5990-5996.
42. W. Siefert, *Thin Solid Films*, 1984, 120, 267-274.
43. A. A. Gentile, C. Rocco, S. Modeo and T. Romano, *J Clean Prod*, 2014, 83, 473-482.
44. Furnaces for Ceramics, Glass, Solar Cells, http://www.thermconcept.com/fileadmin/dokumente/Furnaces_for_Ceramic_Glass_Solar_eng.pdf, Accessed December 2014.
45. SINGLE CHAMBER UNITS, http://bluewaveinc.com/single-chamber-ultrasonic-cleaner/, Accessed December 2014.
46. Desk-Top Automatic Ultrasonic Spray Pyrolysis Coating Equipment (150 X 150mm) - MSK-USP-02, http://www.mtixtl.com/UltrasonicSprayPyrolysis-1.aspx, Accessed December 2014.
47. Screen Printer, http://www.dyesol.com/media/wysiwyg/Documents/equipment-pagers-and-catalogue/2013%20Dyesol%20Catalogue%20005.22042013%20-%20Screen%20Printer.pdf, Accessed December 2014.
48. J. B. Guinée, M. Gorrée, R. Heijungs, G. Huppes, R. Kleijn, A. d. Koning, L. v. Oers, A. Wegener Sleeswijk, S. U. d. H. Suh, H.A., H. d. Bruijn, R. v. Duin and M. A. J. Huijbregts, *Handbook of Life Cycle Assessment: Operation Guide to ISO Standards*, Kluwer Academic Publishers, Secaucus, NJ, USA, 2002.
49. S. Solomon, *The physical science basis: Contribution of Working Group I to the fourth assessment report of the Intergovernmental Panel on Climate Change*, Cambridge University Press, 2007.
50. M. Goedkoop and R. Spriensma, *The eco-indicator99: A damage oriented method for life cycle impact assessment: Methodology report*, PRé Consultants B.V., 2001.
51. E. A. Alsema and E. Nieuwlaar, *Energ Policy*, 2000, 28, 999-1010.
52. V. M. Fthenakis, H. C. Kim and E. Alsema, *Environ Sci Technol*, 2008, 42, 2168-2174.
53. M. A. J. Huijbregts, L. J. A. Rombouts, S. Hellweg, R. Frischknecht, A. J. Hendriks, D. Van de Meent, A. M. J. Ragas, L. Reijnders and J. Struijs, *Environ Sci Technol*, 2006, 40, 641-648.

54. R. Laleman, J. Albrecht and J. Dewulf, *Renew Sust Energ Rev*, 2011, 15, 267-281.
55. D. Y. Liu, J. L. Yang and T. L. Kelly, *J Am Chem Soc*, 2014, 136, 17116-17122.
56. A. Y. Mei, X. Li, L. F. Liu, Z. L. Ku, T. F. Liu, Y. G. Rong, M. Xu, M. Hu, J. Z. Chen, Y. Yang, M. Gratzel and H. W. Han, *Science*, 2014, 345, 295-298.
57. M. Jorgensen, K. Norrman and F. C. Krebs, *Sol Energ Mat Sol C*, 2008, 92, 686-714.
58. P. V. Kamat, *J Phys Chem Lett*, 2013, 4, 3733-3734.
59. V. Fthenakis, *Renew Sust Energ Rev*, 2009, 13, 2746-2750.
60. R. Tipnis, J. Bernkopf, S. Jia, J. Krieg, S. Li, M. Storch and D. Laird, *Sol Energ Mat Sol C*, 2009, 93, 442-446.
61. C. A. Wolden, J. Kurtin, J. B. Baxter, I. Repins, S. E. Shaheen, J. T. Torvik, A. A. Rockett, V. M. Fthenakis and E. S. Aydil, *J Vac Sci Technol A*, 2011, 29, 030801.
62. R. Frischknecht, N. Jungbluth, H.-J. Althaus, R. Hischier, G. Doka, R. Dones, T. Heck, S. Hellweg, G. Wernet and T. Nemecek, *Overview and methodology. Data v2. 0 (2007). Ecoinvent report No. 1*, Ecoinvent Centre, Swiss Federal Laboratories for Materials Testing and Research (EMPA), Duebendorf (Switzerland), 2007.
63. Oracle Crystal Ball, http://www.oracle.com/us/products/applications/crystalball/overview/index.html, Accessed December 2014.
64. D. Smith, *Thin-Film Deposition: Principles and Practice*, McGraw-Hill Education, 1995.
65. K. S. Sree Harsha, in *Principles of Vapor Deposition of Thin Films*, ed. K. S. S. Harsha, Elsevier, Oxford, 2006, DOI: http://dx.doi.org/10.1016/B978-008044699-8/50002-4, pp. 11-143.
66. A. Akcil and S. Koldas, *J Clean Prod*, 2006, 14, 1139-1145.
67. F. C. Krebs, N. Espinosa, M. Hosel, R. R. Sondergaard and M. Jorgensen, *Adv Mater*, 2014, 26, 29-39.